Macromolecules 1983, 16, 1744–1753

Molecular Dynamics of Polycarbonate–Diluent Systems: Applications of High-Resolution Carbon-13 Solid-State NMR

L. A. Belfiore,[+] P. M. Henrichs,[†] D. J. Massa,[†] N. Zumbulyadis,[†] W. P. Rothwell,[‡] and S. L. Cooper*

Department of Chemical Engineering, University of Wisconsin, Madison, Wisconsin 53706.

Received September 15, 1982

ABSTRACT: The effect of low molecular weight miscible additives on the chain dynamics of bisphenol-A polycarbonate (BPAPC) in the glassy state was studied by using high-resolution carbon-13 NMR. The spin–lattice relaxation times in the laboratory frame (T_1) and in the rotating frame ($T_{1\rho}$) were measured at 25 °C for the nonequivalent natural-abundance ^{13}C nuclei in the macromolecule under magic-angle sample spinning conditions. When polycarbonate is blended with diluents having a relatively low glass transition temperature (T_G), such as dibutyl succinate and dibutyl phthalate, $T_{1\rho}$ is decreased substantially at the aromatic and aliphatic carbon locations in the polymer. This results from an increase in the spectral density of micro-Brownian motions in the blends on the order of 50 (or 60) kHz. In contrast, $T_{1\rho}$ remains approximately constant when BPAPC is physically stiffened by the addition of the higher T_G diluents diphenyl phthalate and dinitrobiphenyl. T_1 studies at 25 °C have focused on the effects of antiplasticization on glassy-state mobility in the megahertz regime. The higher T_G diluents suppress the 50-MHz component of the spectral density of thermal motions associated with the sub-T_G (β) relaxation process in the polymer. Of the carbons in BPAPC whose relaxation behavior can be differentiated by high-resolution solid-state NMR, the spin–lattice relaxation times of the protonated aromatic carbons are most highly correlated with the plasticization vs. antiplasticization action of the diluent.

Introduction

A. Polycarbonate–Diluent Interactions. The molecular origin of relaxations in glassy polymers is still the subject of much discussion. The early reviews of Heijboer[1] and Boyer[2] were aimed at addressing the important question of the relationship between chemical structure and the dynamic mechanical properties of selected polymeric glasses. Other studies of molecular motion in the glassy state included effects produced by the addition of low molecular weight miscible diluents to amorphous polymers. The work of Ghersa[3] on poly(vinyl chloride) and Jackson and Caldwell[4–6] on several polycarbonates showed that certain small molecules, referred to as antiplasticizers, have complex effects on the mechanical properties of the host polymer. Whereas the glass transition temperature (T_G) of the macromolecule is depressed by the diluent, an increase in Young's modulus of elasticity is observed. The term "antiplasticization" is used to describe the rigidity and brittleness which developed in these glassy polymer–diluent blends relative to the undiluted polymer.[4]

The use of dynamic mechanical and dielectric relaxation experiments has led to a better understanding of molecular relaxation processes in polymer–diluent systems. Petrie et al.[7] suggested that mobility in both the polymer and the diluent must be considered to develop a complete picture of diluent effects on the physical properties of amorphous polymers below T_G. Petrie defined the temperature ranges of plasticization and antiplasticization for several diluents in polycarbonate and polystyrene. Kinjo[8] studied antiplasticization from a rheological viewpoint. The temperature and additive concentration dependencies of the physical stiffening process in poly(vinyl chloride)–diluent systems were followed using tensile stress relaxation experiments. Kinjo et al.[9] have also discussed their results in terms of diluent effects on both the primary (T_G) and secondary (β) relaxations in PVC. Recently, Seymour et al.[10] observed a new loss process in plasticized cellulose esters. The characteristics of this new mode of molecular motion were found to depend on the flexibility and concentration of the additive molecules. Some approaches have combined dynamic mechanical and dielectric spectroscopies. One might argue that if motional processes differ in their dielectric and mechanical loss intensity, then it is possible to obtain site-specific information on the polar vs. nonpolar aspects of the molecular relaxation process. Locati and Tobolsky[11] have applied this concept in their study of the secondary (β) transition in substituted polycarbonates. In this case, the use of both types of molecular relaxation experiments has verified the cooperative nature of macromolecular motions in the glassy state.

The above-mentioned approaches to solid-state problems in polymer chain dynamics have been described in terms of an overall view of segmental mobility. However, the techniques such as mechanical relaxation fail to relate motion to specific sites in the polymer chain. In this respect, the goal of the present study was to determine how a variety of low molecular weight miscible additives affect macromolecular motions in the glassy state.

B. NMR Spin–Lattice Relaxation in Glassy Polymers. It is well-known and understood that the presence of molecular motion gives rise to relaxation or decay of NMR magnetization.[12] The spin–lattice relaxation time, T_1, and the spin–lattice relaxation time in the rotating frame, $T_{1\rho}$, have been used previously to characterize motions in polymeric solids.[13–17] At ambient temperature, Schaefer et al.[13,18] have shown that carbon-13 $T_{1\rho}$'s of several glassy polymers, including polycarbonates, are dominated by spin–lattice relaxation between 20 and 60 kHz. Hence, the use of $T_{1\rho}$ as a motional parameter is justified within this range of probe frequencies. In the megahertz regime, it is accepted unequivocally that T_1 is completely spin–lattice or motional in orgin.

For heteronuclear spin, I = ^{13}C and S = ^{1}H coupled by a dipolar interaction, the ^{13}C spin–lattice relaxation time in the laboratory frame has been derived in terms of the spectral densities, $J^{(q)}(\omega)$, in the following form:[12,19]

$$\frac{1}{T_1} = \frac{3}{4}\hbar^2\gamma_I^2\gamma_S^2\left\{\frac{1}{12}J^{(0)}(\omega_I-\omega_S)+\frac{3}{2}J^{(1)}(\omega_I)+\frac{3}{4}J^{(2)}(\omega_I+\omega_S)\right\} \quad (1)$$

[+] Present address: Colorado State University, Fort Collins, CO 80523.

[†] Eastman Kodak Co., Rochester, NY 14650.

[‡] Shell Development Co., Westhollow Research Center, Houston, Texas 77001.

0024-9297/83/2216-1744$01.50/0

where γ is the gyromagnetic ratio, ω ($=\gamma H_0$) is the Larmor precession frequency of the spins about the static field (H_0) in the laboratory reference frame, and $\hbar$ is Planck's constant divided by 2π. In this study, ω_S was 200 MHz for ^{1}H and ω_I was 50.3 MHz for ^{13}C nuclei. T_1 is most sensitive to $J^{(1)}(\omega_I)$, which measures the Fourier component of thermal fluctuations at approximately 50 MHz.

Jones[20] has derived an expression for $T_{1\rho}$ assuming a dipolar interaction between homonuclear spins in the weak-collision limit ($T_{1\rho}$ much longer than the correlation time τ_c). At resonance

$$\frac{1}{T_{1\rho}} = \frac{9}{32}\gamma^4\hbar^2\{J^{(0)}(2\omega_e) + 10J^{(1)}(\omega) + J^{(2)}(2\omega)\} \qquad (2)$$

where ω_e is the Larmor frequency (kilohertz regime) about the effective magnetic field in the rotating frame. $T_{1\rho}$ is most sensitive to $J^{(0)}(2\omega_e)$. Menger et al.[17] have derived a ^{13}C $T_{1\rho}$ expression assuming both isotropic random orientation of dipolar-coupled C–H vectors and a rotating-frame Larmor frequency (ω_e for ^{13}C) much smaller than either ω_I or ω_S. In this case, the most important contribution to $T_{1\rho}$ comes from spectral densities evaluated at the single quantum transition frequency ω_e of the observed spins. Contributions in the megahertz regime are also possible theoretically but are insignificant. As a first-order approximation, the effect of magic-angle sample spinning on $T_{1\rho}$ has also been ignored.

In bisphenol-A polycarbonate (BPAPC), the results of dynamic mechanical and dielectric relaxation studies indicate that there are at least two prominent motional processes (primary (T_G) and secondary (β) relaxations) which might contribute to carbon-13 $T_{1\rho}$ relaxation at 25 °C. In this respect, the mid-kilohertz components of the BPAPC spectral density functions probably contain contributions from thermal motions which are, on the average, "fast" (β-relaxation) and "slow" (glass transition) compared to 50 kHz. This is described best by a distribution of correlation frequencies,[21] although Henrichs[22] has suggested that a single molecular process might also contain a large number of correlation frequencies. Steger et al.[14] have concluded that the broad distribution of cooperative main-chain motions of the phenyl groups in BPAPC is composed largely of components whose correlation frequencies (ν_c) are on the order of 10^5 Hz or higher at ambient temperature. This was determined from the weak dependence of $T_{1\rho}$ on the ^{13}C Larmor frequency in the rotating frame (between 20 and 60 kHz). The implication is that the majority of the correlation times which characterize random thermal motions of the phenyl groups in polycarbonate at 25 °C is on the short correlation time side of the minimum in $T_{1\rho}$($\nu_c \sim$ 50 kHz) and the long correlation time side of the minimum in T_1($\nu_c \sim$ 50 MHz). The results of Belfiore et al.[23] reveal that $T_{1\rho}$ at 28 kHz for the protonated aromatic carbons in BPAPC is insensitive to temperature changes between −90 and 20 °C. This also suggests that an accurate description of phenyl group motions requires a broad distribution of correlation frequenices if $T_{1\rho}$ is truly sampling BPAPC chain motions in this regime of temperature and frequency. On the other hand, $T_{1\rho}$ of the phenyl carbons in the polymer increases as the temperature is decreased when BPAPC is blended with the relatively low-T_G diluent dibutyl phthalate. This argues for a narrowing of the distribution of correlation frequencies describing phenyl ring motion in the polymer–diluent blend, which is predominantly on the long correlation time side of the $T_{1\rho}$ minimum at 28 kHz. However, a change in T_1 or $T_{1\rho}$ might arise from a change either in the distribution of correlation frequencies or in the distribution of motional amplitudes. On the basis of the experimental results in this paper, one cannot distinguish between these two possibilities. This is due, in part, to the complexity of the systems studied and the lack of a correlation function model that accounts for motional modulation of both intramolecular and intermolecular ^{1}H–^{13}C dipolar interactions. In this respect, the spin–lattice relaxation time data are discussed solely in terms of the spectral density of micro-Brownian motions in the glassy state.

Experimental Section

A. NMR $T_{1\rho}$ Experiments. High-resolution proton-enhanced ^{13}C NMR spectra in the solid state were obtained with a Bruker CXP-200 commercial spectrometer (Shell Development Co.) and a laboratory-constructed instrument (Eastman Kodak Co.) operating at 200 MHz for ^{1}H (50.3 MHz for ^{13}C) with an Oxford magnet.[24] The 90° pulse width for ^{1}H was either 4.0 or 4.5 μs. Carbon-13 rotating-frame spin–lattice relaxation experiments at 50 (and 60) kHz were performed by using the methodology of Schaefer et al.[13] in the presence of magic-angle sample spinning (MASS) at approximately 4.5 kHz. The strength of the ^{13}C radio-frequency field (H_1) was determined by two independent methods. First, the radio-frequency power in the carbon channel was varied until the ^{13}C signal intensities of adamantane via cross polarization (CP) were maximized. In this case, the 90° pulse width (as well as the magnitude of the H_1 field in frequency units) for ^{13}C was assumed to be the same as that for ^{1}H. In light of the oscillatory behavior of the CP-MASS resonance intensities in adamantane,[25] the ^{13}C 90° pulse width was also measured directly. After cross polarization of the carbons (^{13}C magnetization is assumed to be generated along the x axis), the time necessary to flip the ^{13}C spins 90° to the $\pm z$ axis was monitored until a null in the carbon spectrum was observed. The time determined by this method was within ±0.2 μs of the ^{1}H 90° pulse width. This ensured that the rotating-frame energy level splittings for ^{1}H and ^{13}C were matched according to the Hartmann–Hahn[26] condition, $(\gamma H_1)_{\text{proton}} = (\gamma H_1)_{\text{carbon}}$.

The ^{13}C free induction decay (FID) was acquired with simultaneous high-power proton decoupling at either 50 or 60 kHz. To obtain spectra with a high signal-to-noise ratio, about 1000 FID's were accumulated by using quadrature detection. The delay time between pulse sequence repetitions was 3 s. Prior to Fourier transformation, each FID contained either (a) 4K time-domain data points or (b) 2K time-domain data points zero filled to 8K. The spectral width was ±10 kHz, and line broadening ranged between 10 and 25 Hz. Following Stejskal and Schaefer,[27] spin-temperature alternation in the rotating frame was used to suppress the buildup of artifacts which may occur in proton-enhanced spectra. The temperature of the probe was not controlled and was assumed to be at ambient conditions.

Some of the ^{13}C $T_{1\rho}$ relaxation curves which were constructed with peak intensities from the high-resolution spectra exhibited substantial scatter or fluctuation. This was most prominent in the relaxation curves of the aromatic carbon magnetization resulting from mechanical instabilities in the rotor used for magic-angle sample spinning. Consequently, the resonance line shapes were artificially broadened and the peak intensities were unreliable for those ^{13}C nuclei with relatively large chemical shift anisotropies. To overcome this difficulty, relaxation curves were constructed by using integrated intensities for some of the carbons. It is also possible that long radio-frequency pulses during the $T_{1\rho}$ experiment were the source of the intensity fluctuations observed in the relaxation curves. In each repetition of the pulse sequence, carbon radio-frequency power was on during the entire spin–lattice relaxation period, which varied from τ = 0.1 to τ = 50 ms, while proton radio-frequency decoupling power was on for 102 ms during data acquisition. In both cases, the duration of the radio-frequency pulses might have caused probe heating substantial enough to produce a mismatch in the Hartmann–Hahn condition during cross polarization. Undoubtedly, this unpredictable mismatch leads to a varying ^{13}C magnetization at the beginning of the spin–lattice relaxation interval. This artifact was most prominent in the relaxation curves of carbons without directly bonded protons where the cross-polarization dynamics are extremely sensitive to

Table I
Glass Transition Temperatures of Low Molecular Weight Additives

diluent	structure	T_G, °C
(1) dibutyl succinate (DBS)	$H_9C_4OOC(CH_2)_2COOC_4H_9$	−105
(2) dibutyl phthalate (DBP)	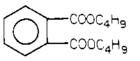	−91
(3) dinitrobiphenyl (DNB)	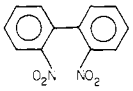	−23
(4) diphenyl phthalate (DPP)	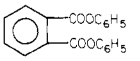	−15

the optimal matched spin-lock conditions.

B. NMR T_1 Experiments. Carbon-13 CP spin–lattice relaxation experiments in the laboratory frame were performed by using a slight modification of the method developed by Torchia.[28] After cross polarization at 50 kHz using a contact time of 2 ms, the ^{13}C magnetization spin-locked along the x axis was rotated 90° to the $-z$ axis, or antiparallel to the static H_0 field. Torchia applied a low-level radio-frequency field to saturate the ^{1}H spins during the entire spin–lattice relaxation interval in order to suppress transient Overhauser effects. In the present work, it was found that this was not necessary, particularly when $T_1(^1H) \ll T_1(^{13}C)$. Fast proton relaxation apparently inhibits a biexponential decay of ^{13}C magnetization without the need for ^{1}H irradiation. The spectral parameters used in the high-resolution (CP-MASS) T_1 experiment were the same as those mentioned above for the $T_{1\rho}$ experiment. It should be mentioned that Torchia's procedure for incorporating spin-temperature alternation into the CP T_1 pulse sequence[28] was not followed in our experiments.

C. Sample Preparation and Physical Property Measurements. Bisphenol-A polycarbonate (BPAPC), obtained from the General Electric Co. as Lexan pellets, was the linear amorphous polymer used in this study. From gel-permeation chromatography using polystyrene standards, the number- and weight-average molecular weights were determined to be 2.7 × 10^4 and 6.0 × 10^4, respectively. The low molecular weight additives, dibutyl phthalate (DBP), dibutyl succinate (DBS), 2,2′-dinitrobiphenyl (DNB), and diphenyl phthalate (DPP), were kindly supplied by Eastman Chemical Products.

BPAPC is known to crystallize in the presence of certain low molecular weight additives that induce plasticization.[29] This process occurs in a limited temperature range above the depressed T_G of the polymer–diluent blend and below the melting point. The sample preparation technique described below was designed to avoid this complication.

Amorphous BPAPC–diluent blends for the stress–strain, DSC, and solid-state NMR experiments were prepared in the following manner: (a) The polymer was dried under vacuum at elevated temperature to remove any traces of moisture. (b) The components of the blend were dissolved in dichloromethane and intimately mixed for at least 24 h. (c) The solvent was removed either by rotary vacuum evaporation in a silicone oil bath at 40 °C or by room-temperature evaporation in a fume hood. (d) The inhomogeneous polymer film was removed from the casting surface, and further solvent removal was conducted at about 75 °C for 10 h. (e) The dried polymer was compression molded at 230 °C for 10 min under a load of about 300 psi to produce a homogeneous blend composition. (f) An ice bath quench was performed slightly above atmospheric pressure. The same procedure was followed in preparing test samples of the undiluted polymer. Wide-angle X-ray diffraction patterns of representative BPAPC–diluent blends ensured the absence of BPAPC crystallinity in all of the materials studied.

Young's modulus of elasticity was measured with an Instron tensile tester at room temperature. Uniaxial elongation was produced by a constant crosshead speed of 2.54 mm/min (0.10 in./min). Samples were initially 6.40 cm (2.50 in.) in length. The initial cross-sectional area was between 0.02 and 0.04 cm^2.

Glass transition temperatures were measured on a DuPont 900 differential thermal analyzer equipped with a DSC cell. The polymeric materials were quenched below T_G from the molten state and then scanned at a heating rate of 20 °C/min. T_G was calculated from the midpoint of the heat capacity difference between the liquid and glassy states. In the vincinity of T_G, no heat capacity overshoot was observed in the thermograms due to relaxation of either enthalpy or uniplanar orientation.

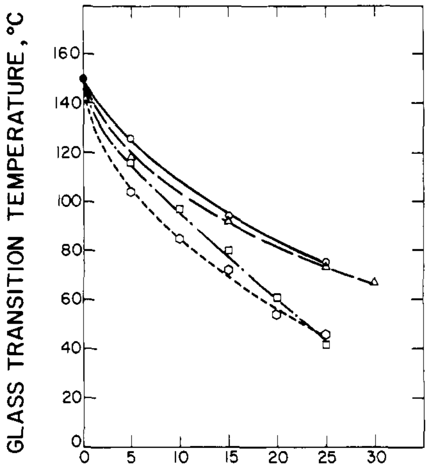

Figure 1. Diluent concentration dependence of the glass transition temperature for polycarbonate–diluent systems: (○) BPAPC–dinitrobiphenyl; (△) BPAPC–diphenyl phthalate; (□) BPAPC–dibutyl phthalate; (○) BPAPC–dibutyl succinate.

Results and Discussion

A. Effect of Diluent T_G on Plasticization vs. Antiplasticization. The glass transition temperatures of the four low molecular weight additives used in this study are given in Table I. Dibutyl succinate and dibutyl phthalate are hereafter referred to as low-T_G diluents whereas diphenyl phthalate and dinitrobiphenyl are referred to as high-T_G diluents.

The effect of additive concentration on the T_G of miscible polymer–diluent blends is illustrated in Figure 1. The undiluted polymer has a glass transition temperature of 150 °C. In all cases, the T_G is lowered by blending a diluent with the polymer. At an equivalent weight (or volume) fraction of diluent, there is a greater depression of T_G in the blends containing the low-T_G diluents. This is in agreement with the results of a simplified free volume theory[30–32] based on a comparison of the glass transition temperatures of the pure diluents.

To establish whether the diluents listed in Table I plasticize (lower Young's modulus of elasticity relative to the undiluted polymer) or antiplasticize (enhance the modulus of) BPAPC at 25 °C, tensile moduli were measured for all BPAPC–diluent blends studied. These data are shown in Figure 2 as a function of the blend glass transition temperature. At the same T_G, the tensile modulus of polycarbonate blended with either dinitrobiphenyl or diphenyl phthalate is greater than that of BPAPC

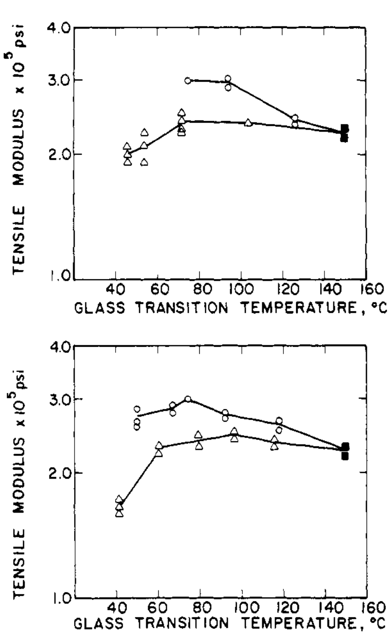

Figure 2. Tensile modulus at 25 °C vs. glass transition temperature for polycarbonate–diluent systems. Top: (○) BPAPC–dinitrobiphenyl; (△) BPAPC–dibutyl succinate. Bottom: (○) BPAPC–diphenyl phthalate; (△) BPAPC–dibutyl phthalate.

containing either dibutyl succinate or dibutyl phthalate. As expected from the dynamic mechanical and dielectric relaxation studies of Petrie et al.,[7] the lower T_G diluents, DBS and DBP, are plasticizers at 25 °C whereas the higher T_G diluents, DPP and DNB, are antiplasticizers at 25 °C. All of the diluents suppress the low-temperature secondary (β) relaxation process in BPAPC, but the lower T_G diluents substantially decrease the blend T_G such that a drop in the room-temperature tensile modulus is observed. There is, however, evidence of a slight stiffening effect in blends containing between 5 and 15 wt % dibutyl phthalate relative to the undiluted polymer. This occurs when the T_G is approximately between 80 and 120 °C. Wyzgoski and Yeh[33] also observed embrittlement in polycarbonate containing 10 wt % DBP. The 90/10 blend of BPAPC and DBP corresponds to the data in Figure 2 (bottom) at a T_G of 97 °C. It appears that the host polymer is not truly plasticized by DBP until the additive concentration exceeds 20 wt % or, equivalently, until the T_G of the blend is less than 60 °C.

The low molecular weight additives listed in Table I were chosen to include an aromatic (DBP) and a nonaromatic (DBS) plasticizer. This allowed us to examine whether the chemical nature of the diluent affects the mobility of the polymer.

B. High-Resolution Solid-State ^{13}C NMR Spectra of Polycarbonate and BPAPC–Diluent Blends. The proton-enhanced dipolar-decoupled ^{13}C NMR spectrum of BPAPC in the solid state is shown in Figure 3A. The dominant resonance in the central region of the spectrum (~89 ppm) is due to the rotor used for magic-angle sample spinning. The rotor is composed of semicrystalline poly(oxymethylene) and is known commercially as Delrin. Five resonance lines are resolved in the solid-state spectrum of the undiluted polymer, and the peak assignments have been made from a comparison with the spectrum of BPAPC in solution[13] shown in Figure 3B. Absolute ^{13}C chemical shifts have also been reported for the solid polymer.[34]

The resonance furthest upfield at 31 ppm (from Me_4Si) is due to the methyl carbons. This signal has an unusually large line width in the MASS spectrum of the solid polymer, which probably can be attributed to methyl groups in a variety of nonequivalent chain conformations. The sharp line at 43 ppm arises from the quaternary carbon in the backbone. Two closely spaced resonances further downfield at 121 and 128 ppm are assigned to the aromatic carbons that have directly bonded protons. Since the spin–lattice relaxation times of all protonated aromatic carbons in BPAPC are almost identical, the data for the resonances at 121 and 128 ppm are reported together. The resonance furthest downfield in the solid-state spectrum is a combination of three nonequivalent carbons, which are distinguishable in the high-resolution spectrum of BPAPC in solution. The two nonprotonated (substituted) aromatic carbon signals at 148 and 149 ppm comprise the majority of the solid line shape. The carbonate ^{13}C resonance at 152 ppm appears as a low-field shoulder and is not well resolved. In this study, the relaxation behavior of the strong downfield resonance at about 150 ppm is attributed solely to the glassy-state mobility of both nonprotonated aromatic carbons. The remaining low-intensity signals in the solid-state spectrum of BPAPC are spinning sidebands of the peaks mentioned above. Since the chemical shifts and peak intensities of the sidebands depend on the sample spinning speed, it was necessary to employ MASS frequencies greater than 3500 Hz at our high-field condition to remove some of the more prominent sidebands from spectral regions of interest.

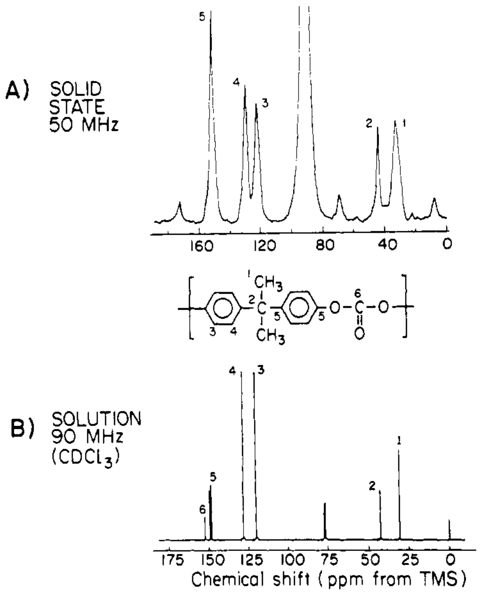

Figure 3. High-resolution carbon-13 NMR spectra of bisphenol-A polycarbonate. The peak assignments are numbered. (A) Solid-state (CP-MASS) spectrum at 50 MHz. The CP contact time is 2 ms. (B) Solution ($CDCl_3$) spectrum at 90 MHz. The spectral parameters for the solution spectrum are 2500 FID's, ^{13}C 90° pulse width = 15 μs, pulse sequence delay time = 3 s, 2-Hz line broadening, and 25 °C.

High-resolution carbon-13 NMR spectra of polycarbonate–diluent blends in the solid state are shown in Figure 4. These spectra are comprised of a superposition of the resonances of each component in the binary mixtures. It is evident that the five resonances of the polymer dominate the spectra of the blends. This is reasonable because the weight ratio of polymer to diluent is approximately 3:1 in each case. The contributions of the diluents result in the following complexities in the blend spectra: (a) polymer resonances are broadened when overlapping line shapes occur (e.g., protonated aromatic signals in the blends containing DBP, DNB, and DPP), and (b) low-intensity signals appear in the regions of the spectrum where no polymer resonances exist (e.g., alipatic peaks of DBP and

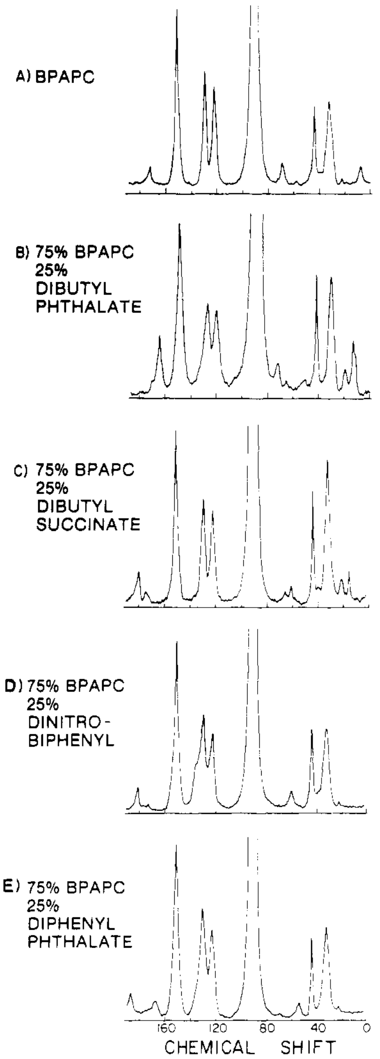

Figure 4. High-resolution carbon-13 NMR spectra of polycarbonate–diluent blends in the solid state: (A) BPAPC; (B) 75% BPAPC–25% dibutyl phthalate; (C) 75% BPAPC–25% dibutyl succinate; (D) 75% BPAPC–25% dinitrobiphenyl; (E) 75% BPAPC–25% diphenyl phthalate.

DBS). Digital subtraction techniques were not utilized to remove the spectral contributions of the diluents.

At ambient temperature, CP-MASS dipolar-decoupled NMR spectra have been obtained for the higher T_G diluents, DNB and DPP, in their pure state.[46] CP-MASS dipolar-decoupled spectra are expected for crystallizable rigid solids below T_M (125 °C for DNB, 70 °C for DPP). However, the lower T_G diluents, DBP and DBS, are above T_M at 25 °C and do not cross polarize. The fact that DBP and DBS resonances are observed in CP spectra of the polymer–diluent blends indicates that strong, near-static ^{1}H–^{13}C dipolar interactions exist within these additive molecules in their mixed state.

In the NMR spectra of the blends, the ^{13}C chemical shifts of BPAPC are not altered by the presence of the low molecular weight component. Based on this result, it does not appear that the formation of charge-transfer complexes between polymer and diluent occurs in the solid state. However, the resolution of the experiment (3–5 ppm for glassy polymers) may not be sufficient to detect relatively small changes in the chemical shift interaction due to charge-transfer effects.

C. Spin–Lattice Relaxation in the Rotating Frame for the Undiluted Polymer. Polycarbonate spin–lattice relaxation curves at 50 kHz are shown in Figure 5 for the five nonequivalent polymer resonances that are resolved in the high-resolution solid state (CP-MASS) NMR spectrum (Figure 3A). From the nonlinearity of each semilogarithmic intensity decay, it is evident that one exponential time constant is not sufficient to completely describe the relaxation behavior of each carbon. In general, a continuous distribution of NMR relaxation times, $\psi(\xi)$, governs the decay of the resonance intensity, $I(\tau)$, in the following manner:

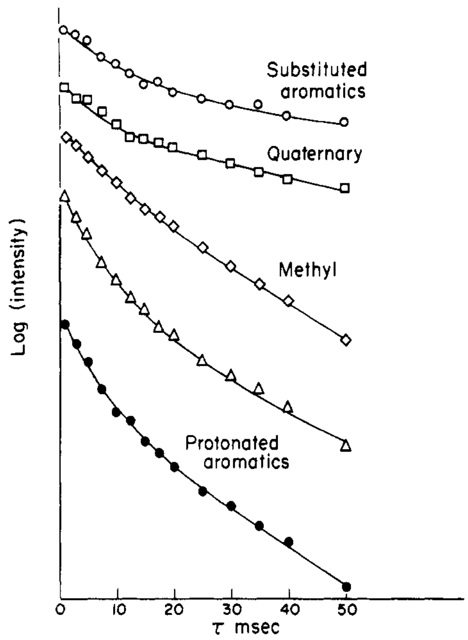

Figure 5. Carbon-13 $T_{1\rho}$ relaxation curves at 50 kHz for the five resonances that are resolved in the solid-state spectrum of BPAPC (Figure 3A). The logarithm of the peak intensity is plotted as a function of the time τ that the carbon magnetization was held in the rotating frame without CP contact with the proton spin system.

$$I(\tau) = \int_0^\infty \psi(\xi)\exp(-\tau/\xi)\,d\xi \qquad (3)$$

In view of the $T_{1\rho}$ curves in Figure 5, the simplest form for $\psi(\xi)$ that can sufficiently model the relaxation behavior is a bimodal δ-function distribution of the form

$$\psi(\xi) = A_1\delta(\xi - \tau_1) + A_2\delta(\xi - \tau_2) \qquad (4)$$

This implies that there are two discrete relaxation times, τ_1 and τ_2. The quantity A_i statistically weights that portion of the relaxation spectrum characterized by τ_i. Since the absolute intensity shown in Figure 5 is arbitrary, the two-time-constant model reduces to

$$I(\tau) = \exp\left\{\frac{-\tau}{T_{1\rho}(\text{short})}\right\} + \phi\exp\left\{\frac{-\tau}{T_{1\rho}(\text{long})}\right\} \qquad (5)$$

where $T_{1\rho}(\text{short}) = \tau_1$, $T_{1\rho}(\text{long}) = \tau_2$, and ϕ ($=A_2/A_1$) is the ratio of the statistical weights for the slow- and fast-decay processes, respectively. The three parameters which adequately describe the relaxation data for each carbon resonance in BPAPC (Figure 5) are given in Table II. The need for at least two relaxation times to characterize each intensity decay (except for the methyl carbon) is a consequence of the dynamical heterogeneity of amorphous polymeric materials below their glass transition temperature.[13]

In BPAPC, the relaxation rates for the protonated aromatic and methyl carbons are faster than those for the quaternary and substituted aromatic carbons. This suggests that modulation of the ^{1}H–^{13}C dipolar couplings provides the major contribution to $T_{1\rho}$ relaxation. This

Table II
Model Parameters Which Characterize the Nonlinear Carbon-13 $T_{1\rho}$ Relaxation Curves at 50 kHz for BPAPC in Figure 5 according to Eq 5

polymer resonance	$T_{1\rho}$(short), ms	$T_{1\rho}$(long), ms	ϕ
substituted aromatic	10 ± 2	131 ± 20	1.08 ± 0.14
quaternary	10 ± 7	84 ± 6	2.51 ± 1.21
methyl		28 ± 2[a]	
protonated aromatics			
121 ppm	6.5 ± 1.5	41 ± 11	0.78 ± 0.30
128 ppm	6.5 ± 1.5	37 ± 9	0.91 ± 0.35

[a] The semilogarithmic intensity decay for this carbon resonance was best fit with a single relaxation time.

is consistent with the results of Schaefer et al.[13] Hence, the nonprotonated (on the 1–4 phenylene axis) and protonated (off axis) aromatic carbons in the polymer have different $T_{1\rho}$'s at 50 kHz even though their motions are described by considering the phenyl group as a single dynamical entity. Inglefield et al.[35] have suggested that this mobility involves phenyl group rotations about the 1–4 phenylene axis. Furthermore, Cheung and Yaris[36] have shown that this rotational motion sweeps out at an angle of at least 8°. In contrast, the conformational calculations of Tonelli[37] on a single isolated BPAPC molecule indicate that a continuum of rotational isomeric states is available to the aromatic rings, with about 1.8 kcal/mol difference between the highest and lowest energy conformers at 25 °C.

One must exercise caution in interpreting the carbon-13 $T_{1\rho}$ as a motional parameter, particularly when strong ^{1}H–^{1}H local fields are present.[38] From the ^{13}C radio-frequency field dependence of $T_{1\rho}$, Schaefer and co-workers[13,18,39] have concluded that the carbon-13 $T_{1\rho}$ at 50 kHz in BPAPC is dominanted by spin–lattice relaxation rather than spin–spin relaxation at ambient temperature. This implies that $T_{1\rho}$ is most sensitive to the spectral density of thermal motions in the mid-kilohertz regime. Thus, we have measured and compared the ^{13}C T_1 and $T_{1\rho}$ of several BPAPC–diluent blends which differ substantially in their macroscopic mechanical and thermal properties. Knowledge of diluent-induced changes in the kilohertz and megahertz motions of BPAPC at ambient temperature will be helpful in evaluating possible mechanisms regarding polymer–diluent interactions. Energy dissipation processes, tensile moduli, impact strength, failure properties, and transport processes may depend strongly on the dynamical state of glassy polycarbonate–diluent blends in these frequency regimes.

D. Spin–Lattice Relaxation in the Rotating Frame for Polycarbonate–Diluent Blends. Polycarbonate–Dibutyl Succinate (DBS). The effect of the low molecular weight low-T_G additive, dibutyl succinate, on the rate of decay of the protonated aromatic ^{13}C magnetization in polycarbonate is illustrated in Figure 6. The rotating-frame relaxation rate, $(T_{1\rho})^{-1}$, of the polymer is enhanced by the presence of the diluent. A similar increase in $(T_{1\rho})^{-1}$ is observed in the methyl region of the polymer as shown in Figure 7. These diluent-induced changes in $T_{1\rho}$ result from an increase in the spectral density of micro-Brownian motions on the order of 50 kHz in both the aromatic and aliphatic regions of the macromolecule.

The relaxation curves in Figure 6 were analyzed with the two-time-constant model given by eq 5. The two relaxation times which characterize the fast [$T_{1\rho}$(short)] and slow [$T_{1\rho}$(long)] components of each nonlinear decay of protonated aromatic carbon magnetization are plotted in Figure 8 as a function of blend T_G. The effect of dibutyl succinate on both $T_{1\rho}$(long) and $T_{1\rho}$(short) for the protonated aromatic carbons in BPAPC is similar. In the 80/20 blend of BPAPC and DBS (T_G = 54 °C), both $T_{1\rho}$(short) and $T_{1\rho}$(long) undergo at least a threefold decrease relative to the corresponding time constants in the undiluted polymer. This suggests that both relaxation times are sensitive to thermal motions of the phenyl groups.

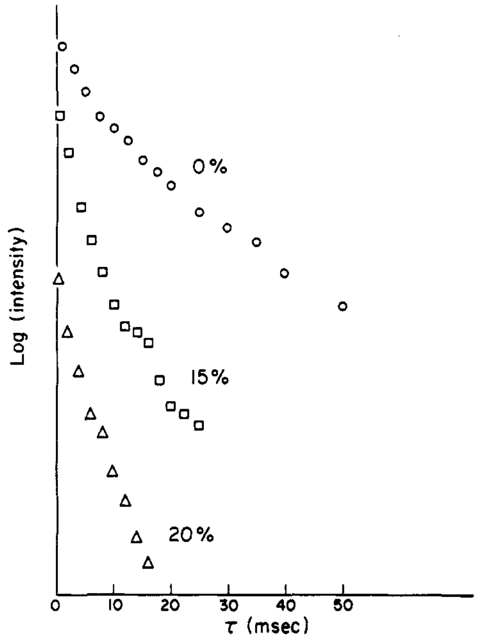

Figure 6. $T_{1\rho}$ relaxation curves at 50 kHz for the protonated aromatic carbons in BPAPC in blends of polycarbonate and dibutyl succinate (DBS). The diluent concentrations in the blends are (○) 0% DBS, (□) 15% DBS, and (△) 20% DBS.

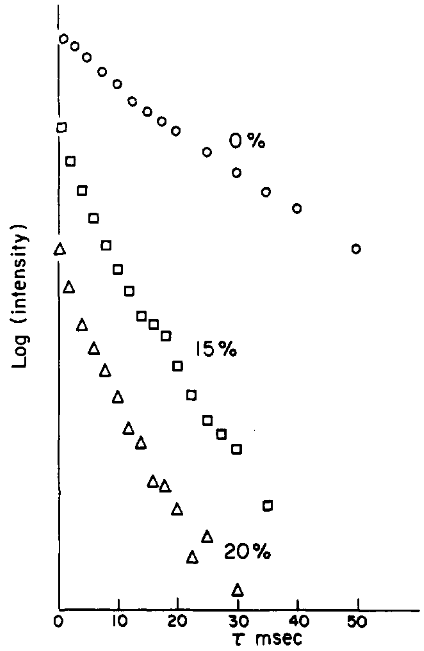

Figure 7. $T_{1\rho}$ relaxation curves at 50 kHz for the methyl carbons in BPAPC in blends of polycarbonate and dibutyl succinate (DBS). The diluent concentrations in the blends are (○) 0% DBS, (□) 15% DBS, and (△) 20% DBS.

$T_{1\rho}$(long) is given in Table III for each nonequivalent carbon site in the polymer (excluding carbonate carbon). The substantial decrease in $T_{1\rho}$ at all locations in the BPAPC molecule implies that DBS enhances the spectral

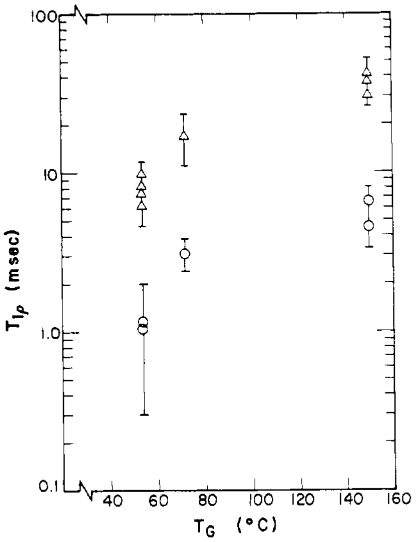

Figure 8. $T_{1\rho}$'s at 50 kHz for the protonated aromatic carbons in BPAPC vs. glass transition temperature for blends of polycarbonate and dibutyl succinate. Both the long and short time constants of each nonlinear intensity decay in Figure 6 are plotted. (△) $T_{1\rho}$(long); (○) $T_{1\rho}$(short).

Table III
Carbon-13 Spin-Lattice Relaxation Times in the Rotating Frame at 50 kHz for Polycarbonate Blended with Dibutyl Succinate[a]

	$T_{1\rho}$(long), ms		
polymer resonance	BPAPC T_G = 150 °C	15% DBS T_G = 72 °C	20% DBS T_G = 54 °C
nonprotonated aromatic	80-151	25-45	22-39
protonated aromatics	26-52	11-23	5-12
quaternary	78-90	25-28	20-28
methyl	26-30	12-16	10-13

[a] For each carbon resonance line, the range of $T_{1\rho}$(long) accounts for (a) the reproducibility determined from repeated experiments on each sample, (b) the uncertainty in fitting the three-parameter nonlinear model (eq 5) using a maximum of 15 data points between τ = 0.1 ms and τ = 50 ms, and (c) the difference in calculating $T_{1\rho}$(long) using both peak and integral NMR intensity decay curves.

density of thermal motions on the order of 50 kHz for the entire repeat unit. Evidence to suport this conclusion in the carbonate regions of BPAPC has been obtained from $T_{1\rho}$ measurements on isotopically labeled polycarbonate without magic-angle sample spinning.[40] The $T_{1\rho}$ data suggest that the effect of dibutyl succinate on BPAPC mobility in the mid-kilohertz regime is not specific to a particular region of the macromolecule. However, it is possible that specific interactions do exist between BPAPC and DBS but that they are obscured by strongly coupled chain dynamics distributed throughout the entire polymer repeat unit.

Polycarbonate–Dinitrobiphenyl (DNB). Polycarbonate spin–lattice relaxation times (slower component) at 50 kHz are given in Table IV for blends of BPAPC and dinitrobiphenyl containing between 0 and 25 wt % DNB. At ambient temperature, the protonated aromatic and methyl carbon $T_{1\rho}$'s are essentially unchanged by the presence of the antiplasticizer. Both $T_{1\rho}$(short) and $T_{1\rho}$(long) for the protonated aromatic carbons are affected similarly. These results imply that dinitrobiphenyl does not significantly alter the spectral density functions describing phenyl group and methyl group mobility in BPAPC on the order of 50 kHz. Furthermore, from $T_{1\rho}$ studies on polycarbonate isotopically labeled at the carbonate carbon,[40] we have confirmed that the spectral density of carbonate group motions at 50 kHz is also unaffected by dinitrobiphenyl.

Table IV
Carbon-13 Spin-Lattice Relaxation Times in the Rotating Frame at 50 kHz for BPAPC in Blends Containing the Higher T_G Diluents[a]

		$T_{1\rho}$(long), ms	
wt % diluent	blend T_G, °C	protonated aromatic	methyl
	BPAPC-Dinitrobiphenyl		
0	150	26-52	26-30
5	126	19-34	27-33
15	94	18-35	24-33
25	75	24-33	24-30
	BPAPC-Diphenyl Phthalate		
0	150	26-52	26-30
5	118	19-28	23-25
15	92	22-36	24-27
25	74	20-55	25-27

[a] The reason for reporting a range of $T_{1\rho}$ is explained in the footnote of Table III.

These results are in agreement with the $T_{1\rho}$ data of Steger et al.[14] for polycarbonate modified by the antiplasticizer Aroclor 1254 (Monsanto Co.). Between 20 and 60 kHz, the rate of decay of the protonated aromatic carbon peak intensities was found to be about 10% slower for the 90/10 blend of BPAPC and the polychlorinated biphenyl relative to that for the undiluted polymer. The difference in the relaxation rates was most evident at longer ^{13}C spin-lock times in the rotating frame (between 5 and 12 ms).

Polycarbonate–Diphenyl Phthalate (DPP). NMR spin–lattice relaxation studies on polycarbonate–diphenyl phthalate blends provide another example where the $T_{1\rho}$'s of the polymer remain approximately constant in the presence of an antiplasticizer. Polycarbonate spin–lattice relaxation times (slower component) at 50 kHz are presented in Table IV for blends of BPAPC and diphenyl phthalate containing between 0 and 25 wt % DPP. The $T_{1\rho}$'s in the blends are not substantially different from their values in the undiluted polymer. The long and short time constants which characterize the nonlinear decay of protonated aromatic carbon magnetization are affected similarly by DPP. The relaxation rate of the methyl carbon magnetization is best described by one time constant in all BPAPC–DPP blends studied. Hence, it is apparent that diphenyl phthalate does not significantly alter the 50-kHz component of the spectral density functions describing micro-Brownian motions in the aromatic and aliphatic regions of the physically stiffened macromolecule.

Polycarbonate–Dibutyl Phthalate (DBP). Comparison with Other BPAPC–Diluent Systems. In this section, results are presented for both plasticized and antiplasticized polycarbonate. The diluent-induced effects on the mid-kilohertz mobility of the polymer are compared and contrasted for BPAPC blended with dibutyl phthalate, dibutyl succinate, or dinitrobiphenyl. $T_{1\rho}$ was measured at a probe frequency of 60 kHz and similarities with the $T_{1\rho}$ results at 50 kHz are cited. The results of Petrie et al.[7] on polycarbonate- and polystyrene-diluent systems suggest that motion associated with the primary (T_G) transition is described by an asymmetric distribution of viscoelastic relaxation times having a low-intensity tail that extends into the mid-kilohertz region. These higher fre-

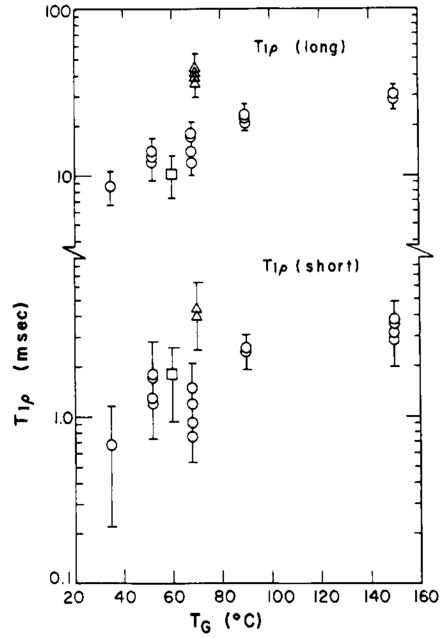

Figure 9. $T_{1\rho}$'s at 60 kHz for the protonated aromatic carbons in BPAPC vs. glass transition temperature for polycarbonate–diluent systems. Both the long and short time constants of each nonlinear intensity decay are plotted. (○) BPAPC–dibutyl phthalate; (△) BAPAC–dinitrobiphenyl; (□) BPAPC–dibutyl succinate.

quency components of motion associated with the onset of T_G may affect $T_{1\rho}$ regardless of whether or not the results of dynamic mechanical and dielectric spectroscopies correlate completely with those from NMR relaxation experiments. In this respect, $T_{1\rho}$'s in different BPAPC–diluent systems are compared at the same blend T_G or at an equivalent temperature interval below T_G.

Diluent effects on $T_{1\rho}$ at 60 kHz are shown in Figure 9 for the protonated aromatic carbons in polycarbonate. Both $T_{1\rho}$(long) and $T_{1\rho}$(short) decrease continuously as the concentration of dibutyl phthalate in the blends is increased (decreasing blend T_G). This implies that DBP enhances the mid-kilohertz mobility of the phenyl groups in BPAPC at ambient temperature. The rate of decay of the protonated aromatic carbon peak intensities at 121 and 128 ppm was analyzed without removing the overlapping resonance contributions from dibutyl phthalate. One might suspect that the relaxation rate of these two carbon resonances in the polymer is affected by the decay of NMR signals due to DBP. With this in mind, $T_{1\rho}$'s of the protonated aromatic carbons at 60 kHz are included in Figure 9 for an 80/20 blend of BPAPC and the low-T_G nonaromatic additive, dibutyl succinate. In this case, the difference between $T_{1\rho}$ in the BPAPC–DBS blend and the undiluted polymer is attributed without reservation to diluent-induced changes in the mid-kilohertz mobility of the phenyl groups in the macromolecule. In the BPAPC–dibutyl phthalate and BPAPC–dibutyl succinate blends that have a T_G of approximately 60 °C, both $T_{1\rho}$(long) and $T_{1\rho}$(short) at 60 kHz for the protonated aromatic carbons are considerably shorter than the corresponding time constants in the undiluted polymer at a T_G of 150 °C (figure 9). This is in agreement with the $T_{1\rho}$ results at 50 kHz for blends of polycarbonate and dibutyl succinate shown in Figure 8. Hence, the mid-kilohertz components of the spectral density functions describing phenyl group mobility in BPAPC are increased by both of the low-T_G diluents.

The low molecular weight additive effects on $T_{1\rho}$(long) at 60 kHz are shown in Figure 10 for the aliphatic carbons in BPAPC. $T_{1\rho}$(long) decreases continuously as the concentration of dibutyl phthalate in the blends is increased. In comparison, the diluent-induced changes in the $T_{1\rho}$'s of the aliphatic carbons are not as substantial as they are for the protonated aromatic carbons (Figure 9) in the same BPAPC–DBP blends.

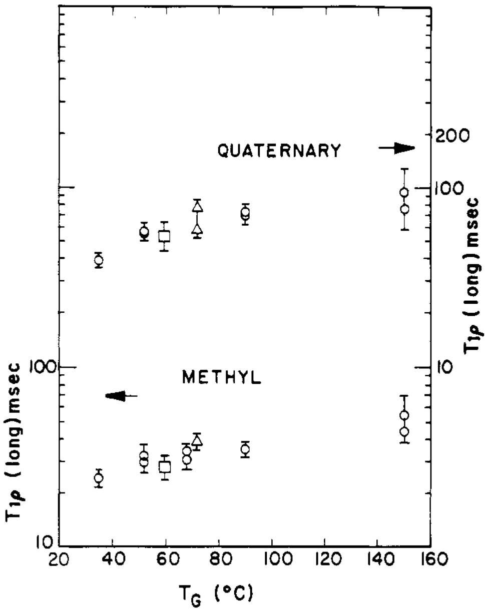

Figure 10. $T_{1\rho}$(long) at 60 kHz for the methyl and quaternary carbons in BPAPC vs. glass transition temperature for polycarbonate–diluent systems. (○) BPAPC–dibutyl phthalate; (△) BPAPC–dinitrobiphenyl; (□) BPAPC–dibutyl succinate.

The data in Figures 9 and 10 indicate that the effects of dibutyl phthalate and dibutyl succinate on polymer $T_{1\rho}$'s are very similar for blends with the same T_G. This suggests that interactions between BPAPC and the low-T_G flexible diluents which enhance the mid-kilohertz mobility of the polymer at 25 °C do not depend on the chemical nature of the diluent. This is consistent with the results of Petrie et al.[7]

In the blend of polycarbonate and dinitrobiphenyl (T_G = 70 °C), $T_{1\rho}$(long) and $T_{1\rho}$(short) at 60 kHz for the protonated aromatic carbons are the same or slightly greater than the corresponding time constants in the undiluted polymer (T_G = 150 °C) as shown in Figure 9. Furthermore, the average values of $T_{1\rho}$(long) and $T_{1\rho}$(short) for the blend of BPAPC and dinitrobiphenyl are more than a factor of 2 greater than the corresponding time constants for the blend of BPAPC and dibutyl phthalate having the same T_G. This implies that the mid-kilohertz mobility of the phenyl groups is substantially different in these two systems. However, for the methyl and quaternary carbons in the polymer, the differences between $T_{1\rho}$(long) in the BPAPC–DNB and BPAPC–DBP blends having a T_G of approximately 70 °C are negligible, as shown in Figure 10.

In Figure 11, $T_{1\rho}$(long) at 60 kHz of the protonated aromatic and methyl carbons is plotted against tensile modulus for BPAPC–dibutyl phthalate and BPAPC–dinitrobiphenyl blends in the glassy state having a T_G below 100 °C. The data suggest that $T_{1\rho}$ of the protonated aromatic carbons is more sensitive to a change in blend tensile modulus than $T_{1\rho}$ of the methyl carbons. Hence, of the ^{13}C nuclei in BPAPC whose relaxation behavior can be differentiated by high-resolution solid-state NMR, $T_{1\rho}$ of the protonated aromatic carbons is most highly correlated with the plasticization vs. antiplasticization action of the diluent. This is reasonable considering the mass and/or moment of inertia of the phenyl groups relative to those of the methyl groups in the macromolecule.

Table V
Carbon-13 Spin-Lattice Relaxation Times T_1 (s) in the Laboratory Frame at 50 MHz for BPAPC in Polycarbonate-Diluent Blends in the Solid State

system	polymer resonance		
	protonated aromatic	quaternary	methyl
polycarbonate	0.37 ± 0.02	1.46 ± 0.04	0.064 ± 0.003
75% polycarbonate-25% dibutyl succinate	0.46 ± 0.02	1.52 ± 0.19	0.063 ± 0.002
70% polycarbonate-30% diphenyl phthalate	0.92 ± 0.18	2.17 ± 0.02	0.066 ± 0.004

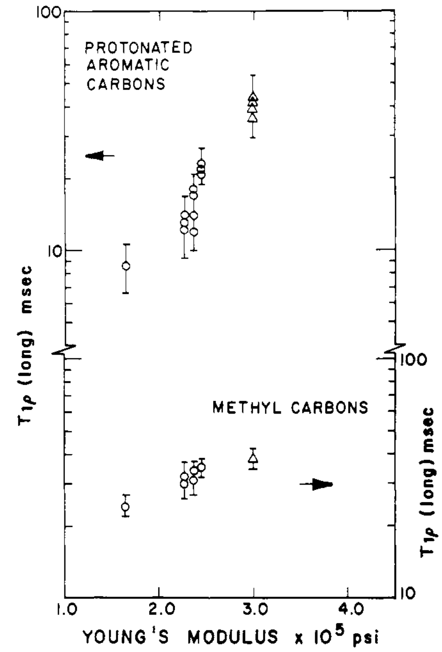

Figure 11. $T_{1\rho}$(long) at 60 kHz for the protonated aromatic and methyl carbons in BPAPC vs. Young's modulus of elasticity for polycarbonate–diluent systems. (○) BPAPC–dibutyl phthalate; (△) BPAPC–dinitrobiphenyl.

One might question a correlation between two motional-related parameters obtained at the same temperature but at different frequencies. Whereas $T_{1\rho}$ was measured at 60 kHz, tensile moduli were measured at an elongation rate of 2.54 mm/min on specimens intially 6.40 cm long, which corresponds to a frequency of about 10^{-4} Hz. A relationship between $T_{1\rho}$ and mechanical or dielectric dissipation factor (tan δ) at the same temperature and frequency would be more consistent. This is demonstrated in a study of diluent effects on the glassy-state mobility of the carbonate group in BPAPC.[40] The relaxation rate of the carbonate ^{13}C magnetization in the rotating frame, $(T_{1\rho})^{-1}$, correlates well with the magnitude of the dielectric dissipation factor in the mid-kilohertz regime at 25 °C. In this case, the concerted mobility of the carbonate group is primarly responsible for the relaxation phenomena observed in each experiment.

E. Spin–Lattice Relaxation in the Laboratory Frame at 50 MHz. It is well-known that the local segmental mobility of a glassy polymer is suppressed by the addition of a low molecular weight miscible diluent which acts as either a plasticer or an antiplasticizer at 25 °C.[7-9] Diluent effects on the sub-T_G (β) relaxation process in BPAPC have been observed by both dynamic mechanical[33,41] and dielectric relaxation[7] experiments. In this section, diluent effects on the megahertz mobility of BPAPC are investigated by using the cross-polarization spin–lattice relaxation experiment in the laboratory frame. At ambient temperature, thermal fluctuations associated with the β-process in polycarbonate give rise to T_1 relaxation.[42] Moreover, the megahertz mobility in BPAPC at 25 °C is not influenced appreciably by the T_G of the system.

The T_1 results presented in Table V were obtained from high-resolution solid-state (CP-MASS) ^{13}C NMR spectra of polycarbonate and BPAPC–diluent blends similar to those shown in Figure 4. T_1 was calculated by using a three-parameter nonlinear model suggested by Peat and Levy[43] in the following form:

$$M_z(\tau) = M_z(\infty) \times \left\{1 - \left[1 - \frac{M_z(0)}{M_z(\infty)}\left\{1 - \exp\left(-\frac{t_d}{T_1}\right)\right\}\right]\exp\left(-\frac{\tau}{T_1}\right)\right\} \quad (6)$$

where t_d is the pulse sequence repetition time. The three parameters obtained by fitting eq 6 to the ^{13}C relaxation data are the initial magnetization $M_z(0)$, the equilibrium magnetization $M_z(\infty)$, and the spin–lattice relaxation time T_1. In all cases, the ratio of $M_z(0)$ to $M_z(\infty)$ is less than the theoretical upper limit of 4 for proton-enhanced ^{13}C magnetization.[44] The uncertainty in T_1 given in Table V results from fitting the three-parameter nonlinear model (eq 6) using a maximum of ten data points between τ = 75 μs and τ = 5 s.

For each carbon resonance listed in Table V, a comparison of the T_1's for polycarbonate and the 75/25 blend of polycarboante and dibutyl succinate indicates that DBS does not substantially affect the spin–lattice relaxation times of the polymer. The difference between the protonated aromatic carbon T_1's of 0.37 ± 0.02 s for the undiluted polymer and 0.46 ± 0.02 s for the blend is considered to be relatively unimportant in this analysis. The data suggest that the plasticizer, dibutyl succinate, does not significantly alter the 50-MHz components of the spectral density functions describing aliphatic and aromatic mobility in BPAPC at ambient temperature.

In contrast, the addition of 30 wt % diphenyl phthalate to BPAPC results in a considerable increase in T_1 at both the protonated aromatic and quaternary carbon sites in the polymer. The relaxation rate of the methyl carbon magnetization is not affected by DPP. This suggests that the antiplasticizing diluent preferentially diminishes the spectral density of 50-MHz motions in the aromatic and quaternary regions of the macromolecule. However, it is difficult to imagine a motion involving the protonated aromatic and quaternary carbons that does not involve the methyl carbons as well. The methyl T_1 is at least an order of magnitude shorter than the other carbon T_1's, which suggests that efficient internal rotation of the methyl groups is the major contributor to its T_1 process. In addition, T_1 studies on BPAPC isotopically labeled at the carbonate carbon[45] have confirmed that the spectral density of carbonate group motions at 50 MHz is substantially diminished by the antiplasticizer 2,2′-dinitrobiphenyl. Hence, the effects of antiplasticization on the local segmental mobility of BPAPC at 25 °C might result from strongly coupled interactions between polymer and diluent distributed throughout the macromolecule in a cooperative manner.

Conclusions

The effects of low molecular weight miscible additives on the glassy-state mobility of bisphenol-A polycarbonate have been studied by using high-resolution carbon-13 NMR spin–lattice relaxation experiments in the rotating frame ($T_{1\rho}$ at 50 kHz and 60 kHz) and in the laboratory frame (T_1 at 50 MHz) at ambient temperature. Diluent-induced changes in T_1 or $T_{1\rho}$ might arise from perturbations either in the distribution of correlation frequencies or in the distribution of motional amplitudes of the random thermal fluctuations which give rise to spin–lattice relaxation. On the basis of the experimental results presented in this paper, one cannot distinguish between these two possibilities. In this respect, the results have been discussed in terms of diluent-induced changes in the spectral density of micro-Brownian motions in the glassy state. The following conclusions may be drawn.

(1) The low-T_G diluents, dibutyl succinate and dibutyl phthalate, enhance the mid-kilohertz mobility of the entire BPAPC molecule at 25 °C. Solid-state interactions between BPAPC and the low-T_g diluents which produce a substantial decrease in polymer $T_{1\rho}$'s do not depend on the chemical nature of the low molecular weight component in the blend. At all carbon locations in the macromolecule, the decrease in $T_{1\rho}$ correlates well with the decrease in blend T_G for the solid solutions containing the low-T_G diluents.

(2) The higher T_G diluents, diphenyl phthalate and dinitrobiphenyl, which are well-known antiplasticizers for BPAPC at 25 °C, have a negligible effect on the mid-kilohertz components of the spectral density functions describing micro-Brownian motions in the macromolecule. The $T_{1\rho}$–T_G correlation mentioned above could not be extended to include the effect of the higher T_G diluents.

(3) A correlation between $T_{1\rho}$ (at 60 kHz) and diluent plasticization vs. antiplasticization is suggested. The $T_{1\rho}$'s of the protonated aromatic carbons in BPAPC are most highly correlated with the diluent-induced changes in the room-temperature tensile moduli in glassy blends having a T_G below 100 °C.

(4) Antiplasticization substantially affects the megahertz mobility of BPAPC at 25 °C associated with the sub-T_G (β) relaxation process. When polycarbonate is blended with the higher T_G diluents, strong interactions between polymer and diluent are distributed throughout the macromolecular repeat unit by cooperative motions in the megahertz regime.

Diluent effects on the solid-state mobility of the carbonate group in BPAPC are reported elsewhere.[40,45]

Acknowledgment. We thank Dr. Dale Holecek (Shell Development Co., Westhollow Research Center) for performing the initial NMR relaxation experiments on our materials. Mr. Stanley Gross (Eastman Kodak Research Laboratories) was primarily responsible for the construction and maintenance of one of the NMR spectrometers. L.A.B. expressed his gratitude for the opportunity to carry out this research at both the Shell Development Co. and the Eastman Kodak Co. This work was supported in part by the Petroleum Research Fund, administered by the American Chemical Society.

Registry No. Bisphenol A polycarbonate (SRU), 24936-68-3; bisphenol A–carbonic acid copolymer, 25037-45-0; dibutyl succinate, 141-03-7; dibutyl phthalate, 84-74-2; diphenyl phthalate, 84-62-8; 2,2′-dinitrobiphenyl, 2436-96-6.

References and Notes

(1) J. Heijboer, *Br. Polym. J.*, **1**, 3 (1969).
(2) R. F. Boyer, *Polym. Eng. Sci.*, **8**, 161 (1968).
(3) P. Ghersa, *Mod. Plast.*, **36**, 135 (1958).
(4) W. J. Jackson and J. R. Caldwell, *Adv. Chem. Ser.*, **No. 48**, 185 (1965).
(5) W. J. Jackson and J. R. Caldwell, *J. Appl. Polym. Sci.*, **11**, 211 (1967).
(6) W. J. Jackson and J. R. Caldwell, *J. Appl. Polym. Sci.*, **11**, 227 (1967).
(7) S. E. B. Petrie, R. S. Moore, and J. R. Flick, *J. Appl. Phys.*, **43**, 4318 (1972).
(8) N. Kinjo, *Jpn. Plast.*, 6, Oct 1973.
(9) N. Kinjo and T. Nakagawa, *Polym. J.*, **4**, 143 (1973).
(10) R. W. Seymour, S. Weinhold, and S. K. Haynes, *J. Macromol. Sci., Phys.*, **B16** (3), 337 (1979).
(11) G. Locati and A. V. Tobolsky, *Adv. Mol. Relax. Processes*, **1**, 375 (1970).
(12) A. Abragam, "The Principles of Nuclear Magnetism", Oxford University Press, London/New York, 1961, Chapter 8.
(13) J. Schaefer, E. O. Stejskal, and R. Buchdahl, *Macromolecules*, **10**, 384 (1977).
(14) T. R. Steger, J. Schaefer, E. O. Stejskal, and R. A. McKay, *Macromolecules*, **13**, 1127 (1980).
(15) M. D. Sefcik, J. Schaefer, E. O. Stejskal, and R. A. McKay, *Macromolecules*, **13**, 1132 (1980).
(16) L. W. Jelinski, F. C. Schilling, and F. A. Bovey, *Macromolecules*, **14**, 581 (1981).
(17) E. M. Menger, W. S. Veeman, and E. de Boer, *Macromolecules*, **15**, 1406 (1982).
(18) J. Schaefer, E. O. Stejskal, T. R. Steger, M. D. Sefcik, and R. A. McKay, *Macromolecules*, **13**, 1121 (1980).
(19) I. Solomon, *Phys. Rev.*, **99**, 559 (1955).
(20) G. P. Jones, *Phys. Rev.*, **148**, 332 (1966).
(21) J. Schaefer, *Macromolecules*, **6**, 882 (1973).
(22) P. M. Henrichs, *J. Polym. Sci., Polym. Phys. Ed.*, **21**, 263 (1983).
(23) L. A. Belfiore, J. R. Lyerla, and S. L. Cooper, *Macromolecules*, submitted for publication.
(24) S. Gross and N. Zumbulyadis, *Rev. Sci. Instrum.*, **53**, 615 (1982).
(25) E. O. Stejskal, J. Schaefer, and J. S. Waugh, *J. Magn. Reson.*, **28**, 105 (1977).
(26) S. R. Hartmann and E. L. Hahn, *Phys. Rev.*, **128**, 2042 (1962).
(27) E. O. Stejskal and J. Schaefer, *J. Magn. Reson.*, **18**, 560 (1975).
(28) D. A. Torchia, *J. Magn. Reson.*, **30**, 613 (1978).
(29) R. Legras and J. P. Mercier, *J. Polym. Sci., Polym. Phys. Ed.*, **17**, 1171 (1979).
(30) H. Fujita and A. Kishimoto, *J. Chem. Phys.*, **34**, 393 (1961).
(31) F. N. Kelley and F. Bueche, *J. Polym. Sci.*, **50**, 549 (1961).
(32) L. J. Garfield and S. E. B. Petrie, *J. Phys. Chem.*, **68**, 1750 (1964).
(33) M. G. Wyzgoski and G. S. Y. Yeh, *Polym. J.*, **4**, 29 (1973).
(34) W. L. Earl and D. L. VanderHart, *J. Magn. Reson.*, **48**, 35 (1982).
(35) P. T. Inglefield, A. A. Jones, R. P. Lubianez, and J. F. O'Gara, *Macromolecules*, **14**, 288 (1981).
(36) T. T. P. Cheung and R. Yaris, *J. Chem. Phys.*, **76** (6), 3604 (1980).
(37) A. E. Tonelli, *Macromolecules*, **5**, 558 (1972).
(38) D. L. VanderHart and A. N. Garroway, *J. Chem. Phys.*, **71**, 2773 (1979).
(39) J. Schaefer, M. D. Sefcik, E. O. Stejskal, and R. A. McKay, *Macromolecules*, **14**, 280 (1981).
(40) L. A. Belfiore, P. M. Henrichs, and S. L. Cooper, *Polymer*, accepted for publication.
(41) L. M. Robeson and J. A. Faucher, *J. Polym. Sci., Polym. Lett. Ed.*, **7**, 35 (1969).
(42) L. A. Belfiore and S. L. Cooper, *J. Polym. Sci., Polym. Phys. Ed.*, in press.
(43) I. R. Peat and G. C. Levy, *J. Magn. Reson.*, **18**, 500 (1975).
(44) A. Pines, M. G. Gibby, and J. S. Waugh, *J. Chem. Phys.*, **59**, 569 (1973).
(45) P. M. Henrichs, D. J. Massa, L. A. Belfiore, and H. Isaacson, to be published.
(46) L. A. Belfiore, unpublished results.